

## OEDGE modeling of $^{13}\text{C}$ deposition in the inner divertor of DIII-D

J.D. Elder <sup>a,\*</sup>, P.C. Stangeby <sup>a,b,c</sup>, D.G. Whyte <sup>d</sup>, S.L. Allen <sup>c</sup>,  
A. McLean <sup>a,b</sup>, J.A. Boedo <sup>e</sup>, B.D. Bray <sup>b</sup>, N.H. Brooks <sup>b</sup>,  
M.E. Fenstermacher <sup>c</sup>, M. Groth <sup>c</sup>, C.J. Lasnier <sup>c</sup>, S. Lisgo <sup>a</sup>,  
D.L. Rudakov <sup>e</sup>, W.R. Wampler <sup>f</sup>, J.G. Watkins <sup>f</sup>, W.P. West <sup>b</sup>

<sup>a</sup> University of Toronto, Institute for Aerospace Studies, 4925 Dufferin St., Downsview, ON, Canada M3H 5T6

<sup>b</sup> General Atomics, P.O. Box 85608, San Diego, CA 92186-5608, USA

<sup>c</sup> Lawrence Livermore National Laboratory, P.O. Box 808, Livermore, CA 94551-0808, USA

<sup>d</sup> University of Wisconsin – Madison, Madison, WI 53706, USA

<sup>e</sup> University of California – San Diego, La Jolla, CA 92093, USA

<sup>f</sup> Sandia National Laboratory, P.O. Box 5800, Albuquerque, NM 87185, USA

### Abstract

Use of carbon in tokamaks leads to a major tritium retention issue due to co-deposition. To investigate this process a low power L-mode experiment was performed on DIII-D in which  $^{13}\text{CH}_4$  was puffed into the main vessel through the toroidally-symmetric pumping plenum at the top of lower single-null discharges. Subsequently, the  $^{13}\text{C}$  content of tiles taken from the vessel wall was measured. The interpretive OEDGE code was used to model the results. It was found that the  $^{13}\text{C}$  deposition pattern is controlled by: (a) source strength of  $^{13}\text{C}^+$ , (b)  $\Delta r_s$ , radial location of the  $^{13}\text{C}^+$  source, (c)  $D_{\perp}$ , (d)  $M_{\parallel}$ , the scrape-off layer parallel Mach number. Best agreement was found for (a)  $\sim 50\%$  conversion efficiency  $^{13}\text{CH}_4 \rightarrow ^{13}\text{C}^+$ , (b)  $\Delta r_s, \sim +3.5$  cm (outboard of separatrix) near  $^{13}\text{CH}_4$  injection location, (c)  $D_{\perp} \sim 0.3$  m<sup>2</sup>/s, (d)  $M_{\parallel} \sim 0.4$  toward inside.

© 2004 Elsevier B.V. All rights reserved.

PACS: 52.65

Keywords: Carbon Impurities; DIII-D; Edge modeling; Impurity transport; OEDGE

### 1. Introduction

The carbon–hydrogen co-deposition process does not saturate and could result in an unacceptable build up of tritium inventory. There are three principal questions: (1) What is the source of the carbon? (2) What transport mechanism carries the carbon in the scrape off layer? (3) What determines the deposition location of the carbon?

\* Corresponding author. Tel.: +1 905 839 8180/416 667 7891; fax: +1 416 667 7799.

E-mail address: [david@starfire.utias.utoronto.ca](mailto:david@starfire.utias.utoronto.ca) (J.D. Elder).

This paper is an interpretive modeling investigation related to the 2nd and 3rd questions.

The injection of  $^{13}\text{CH}_4$  into the edge of tokamaks has been shown on TEXTOR [1] and JET [2] to provide valuable opportunities for diagnosis of carbon behaviour. On DIII-D a well-controlled low power,  $\sim 1$  MW, Simple As Possible Plasma (SAPP) L-mode experiment was run in which  $^{13}\text{CH}_4$  was puffed through the upper pumping plenum of lower single-null (LSN) discharges [3]. This puff was toroidally symmetric and at a rate which did not significantly perturb the local plasma conditions (determined by examination of several plasma diagnostics). The puff rate was limited so that the increase in the measured carbon density in the core was modest,  $\sim 35\%$ . The  $^{13}\text{C}$  was puffed for 22 consecutive identical discharges for a period of 3 s during each discharge under steady-state plasma conditions. There were He glow conditioning discharges, with a duration of 5 min, between each of the main discharges. Immediately after this experiment, DIII-D was vented and 29 tiles were removed for analysis. The  $^{13}\text{C}$  content of the tiles was measured using nuclear reaction analysis [4]. For these conditions, detectable  $^{13}\text{C}$  deposition was only found for tiles in the inner divertor region.

The Osm Eirene Divimp edge (OEDGE) code [5] was used in this study to model the transport and deposition of the  $^{13}\text{C}$ . The objective was to identify and quantify the controlling factors governing the  $^{13}\text{C}$  deposition pattern. It is found that the  $^{13}\text{C}$  deposition pattern and core  $^{13}\text{C}$ -content are essentially controlled by four quantities: (a) the source strength of  $^{13}\text{C}^+$ , (b)  $\Delta r_s$ , the radial location of the  $^{13}\text{C}^+$  source, (c)  $D_\perp$ , (d)  $M_\parallel$ , the parallel Mach number. Large values of  $M_\parallel$  toward the inside, in the scrape-off layer (SOL) at the top (LSN divertor), have been measured in a number of tokamaks, but attempts to explain/model this flow have been unsuccessful to date. Separately reported OEDGE analysis [6] is used to model (a) and (b). Here all four control parameters are treated as unknowns and the range of their permitted values is ‘backed’ out of the interpretive code analysis by comparison with the experimental measurements.

## 2. Results

The first step in the OEDGE analysis was to use all available experimental data and the ‘onion-skin’ modeling (OSM) in OEDGE to infer a solution for the background plasma by empirical reconstruction. (There is insufficient space in the present paper to adequately describe this modeling method, but a very similar reconstruction exercise, also for a detached DIII-D divertor case, is reported in these proceedings [7].) This plasma solution (identified as OSM in the figures) is then used as the basis for calculating the transport and deposition of the  $^{13}\text{C}$  in the rest of the study. The experimental data

used here included calibrated spectroscopic measurements of  $D_\alpha$ ,  $D_\beta$  and  $D_\gamma$  for both the inner and outer targets, target Langmuir probe measurements of  $I_{\text{sat}}^+$ , and upstream measurements of the plasma profiles. The plasma solution obtained by this empirical modeling used the Langmuir probe  $I_{\text{sat}}^+$  as input (Fig. 1).

The solution matched the hydrogenic spectroscopy (EIRENE-calculated profiles) (Fig. 2) at the inner and outer targets as well as the upstream plasma measurements (Fig. 3). The inner target was found to be detached with a near target plasma temperature of  $0.8 \pm 0.2$  eV. The  $D_\alpha$ ,  $D_\beta$ ,  $D_\gamma$  are extremely sensitive ‘ $T_e$  thermometers’ in these cold, dense conditions, providing most valuable, and precise, input to the empirical reconstruction of the inner plasma, see Ref. [7]. Superimposed by the code on the plasma solution was a parallel plasma flow of specified Mach number,  $M_\parallel$ , extending from near the outer target to near the inner one.  $M_\parallel \equiv v_\parallel / [(T_e + T_i)/m_D]^{1/2}$ ,  $T_i = T_e$  assumed.

The  $^{13}\text{C}$  deposition measurements found no significant  $^{13}\text{C}$  deposition (above background) anywhere other than the inner target region. The experimental deposition is shown with the model results below.

Studies varying  $D_\perp$  from 0.05 to 1.0 and  $M_\parallel$  from 0.05 to 2.0 independently were performed. The deposition patterns from these simulations were compared to the experimental values. It was found that the carbon core edge density  $n_e^{\text{sep}}$  was particularly important in identifying which combinations of parameters appropriately replicated the observed experimental deposition. The simulation results presented here were selected from the larger set to demonstrate the effects of changing parameter values.

A series of simulations were run where the parallel flow was specified, radially constant, varying from  $M_\parallel = 0.05$  up to  $M_\parallel = 2$ , all with  $D_\perp = 0.3$  m<sup>2</sup>/s.  $^{13}\text{C}$  was launched in DIVIMP as  $^{13}\text{C}^+$  at the top of the torus, with  $\Delta r_s = +3.6$  cm (perpendicular distance from the separatrix). The calculated  $^{13}\text{C}$  deposition patterns are

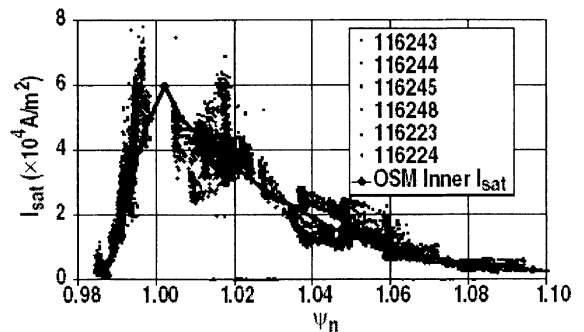


Fig. 1. Comparison of Langmuir probe  $I_{\text{sat}}$  and OSM input  $I_{\text{sat}}$ , inner target.  $\Psi_n$  is the normalized poloidal flux magnetic coordinate.

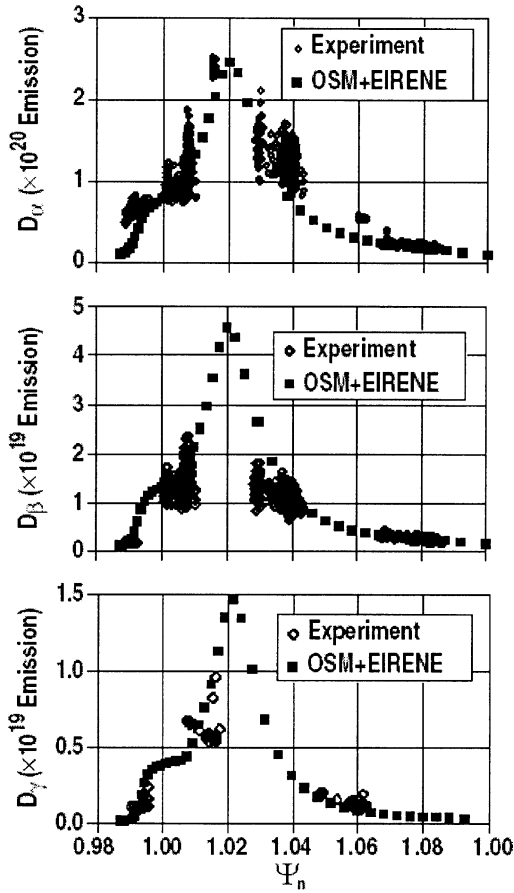


Fig. 2. (a–c) Comparison of the experimental and modeled  $D_{\alpha}$ ,  $D_{\beta}$  and  $D_{\gamma}$  spectroscopy at inner target. Units of photons/m<sup>2</sup>/s/sr. The modeled hydrogen spectroscopy is produced by EIRENE using the OSM plasma solution as input. This identified the value of  $T_e$  at the inner target as  $\sim 0.8 + 0.2$  eV.

shown in Fig. 4. The experimental profile is best matched by  $M_{\parallel}$  of  $\sim 0.4$ . If the flow in the SOL is too slow the deposition spreads out on the inner target and significant deposition is seen on the inner wall – contrary to observation. If the SOL flow is too fast then the deposition profile on the inner target becomes too narrow. This result indicates that the SOL flow lies in the range  $M_{\parallel} = \sim 0.3–0.6$  directed toward the inside. Assumption of flow, at any speed, toward the outside completely fails to match the measured deposition pattern. In the next study the parallel flow was fixed at  $M_{\parallel} = 0.4$  with the same  $C^+$ -source location ( $\Delta r_s = +3.6$  cm), while the value of  $D_{\perp}$  was varied. Results are shown in Fig. 5. In this case, smaller values of  $D_{\perp}$  cause the target deposition profile to become more peaked while the larger  $D_{\perp}$  values spread the deposition out across the target. The larger values of  $D_{\perp}$  give more deposition on the inner wall. The transport is dominated

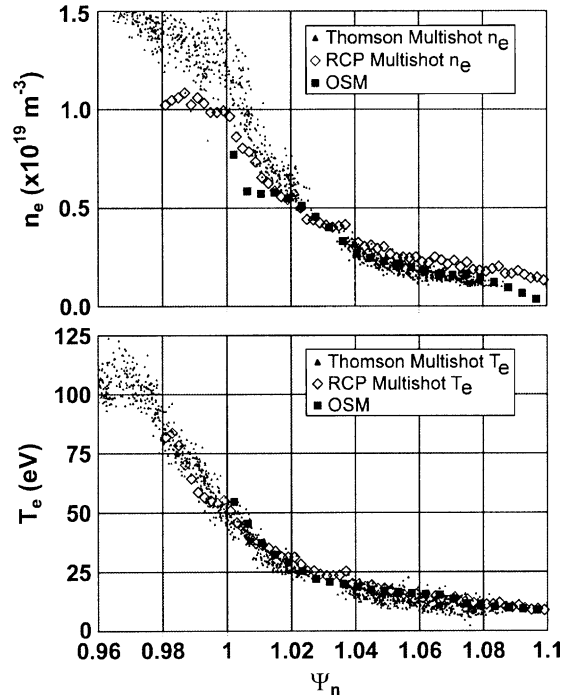


Fig. 3. Comparison of upstream  $n_e$  and  $T_e$  for Thomson (TS), reciprocating probe (RCP) and the OSM solution. The TS and RCP profiles did not line up exactly, perhaps due to uncertainties in identifying the separatrix locations, and were slightly shifted (Thomson outward by  $0.01 \Psi_n$  and RCP inward by  $0.03 \Psi_n$ ) to match the OSM result. The OSM profiles are essentially based on the target plasma conditions, where the location of the separatrix may be easier to identify, e.g. from the peak in the  $I_{sat}$  profile, Fig. 1.

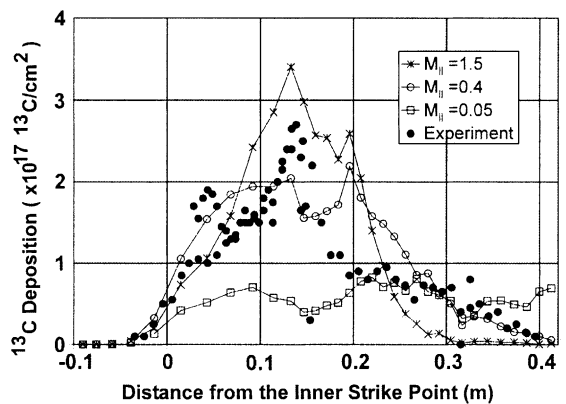


Fig. 4. Deposition as a function of  $M_{\parallel}$  – the parallel flow Mach number. Distance from inner strike point is toward inside of the tokamak, smaller  $R$ .

by the parallel flow. It is concluded that  $D_{\perp} \sim 0.3–0.5$  m<sup>2</sup>/s. In the next study, <sup>13</sup>C ions were started at

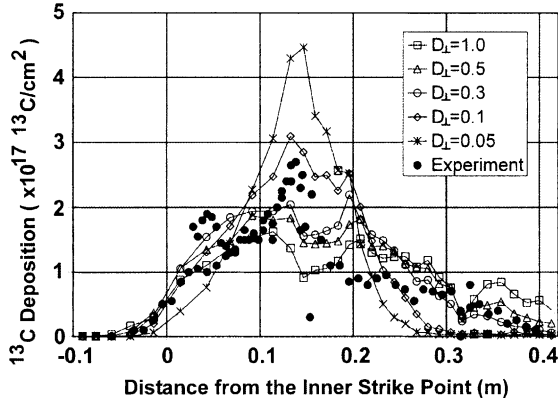


Fig. 5. Deposition as a function of  $D_{\perp}$ .

different radial ( $\Delta r_s$ ) locations upstream.  $M_{\parallel} = 0.4$ ,  $D_{\perp} = 0.3 \text{ m}^2/\text{s}$ . The launch locations varied from inside the separatrix ( $-\vee \Delta r_s$ ) to the middle of the SOL. Results are shown in Fig. 6. Starting too far out in the SOL results in significant inner wall deposition and a target deposition peak located too far from the inner strike point. On the other hand, a source too close to the separatrix moves the deposition peak inward toward the strike point. It is concluded that the  $^{13}\text{C}^+$  source is located at  $\Delta r_s = +3\text{--}6 \text{ cm}$ . From the comparisons in Figs. 4–6, a conversion efficiency of  $\sim 50 \pm 20\%$  was inferred (this value was used for scaling the code results). This value was inferred by matching the magnitude of the calculated deposition to the measured amount – an upstream ion source with a magnitude of  $\sim 50\%$  of the known total influx of  $^{13}\text{CH}_4$ ; was sufficient to match the measured deposition. Raising or lowering the efficiency simply changes the amount of the calculated deposition.

The increment in the carbon ion density at the separatrix,  $\Delta n_c^{\text{sep}}$ , places an additional and key constraint on

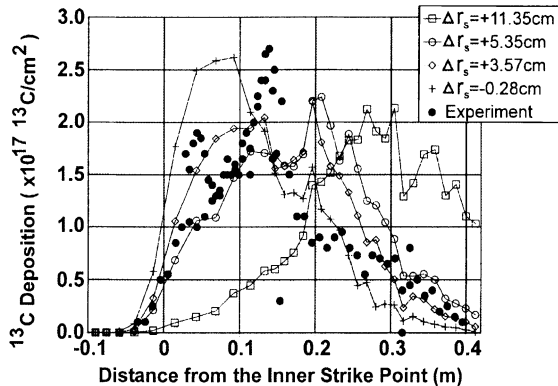


Fig. 6. Deposition as a function of initial  $^{13}\text{C}^+$  radial position,  $\Delta r_s$ , relative to the separatrix.

Table 1

Increment in the density of carbon ions just inside the core plasma,  $\Delta n_c^{\text{sep}}$ , for a range of simulation conditions

Case $M_{\parallel}$	$\Delta n_c^{\text{sep}}$ ( $\text{C}/\text{m}^3$ )	Case $D_{\perp}$	$\Delta n_c^{\text{sep}}$ ( $\text{C}/\text{m}^3$ )
$M = 2.0$	$1.40\text{E}+15$	$D_{\perp} = 1.0$	$2.59\text{E}+16$
$M = 1.5$	$2.94\text{E}+15$	$D_{\perp} = 0.5$	$2.58\text{E}+16$
$M = 1.0$	$6.25\text{E}+15$	$D_{\perp} = 0.3$	$2.61\text{E}+16$
$M = 0.9$	$8.74\text{E}+15$	$D_{\perp} = 0.1$	$1.40\text{E}+16$
$M = 0.8$	$9.74\text{E}+15$	$D_{\perp} = 0.05$	$4.50\text{E}+15$
$M = 0.7$	$1.19\text{E}+16$		
$M = 0.6$	$1.50\text{E}+16$	$\Delta r_s$ (cm)	
$M = 0.5$	$1.93\text{E}+16$	11.35	$9.36\text{E}+14$
$M = 0.4$	$2.61\text{E}+16$	9.22	$2.92\text{E}+15$
$M = 0.3$	$3.66\text{E}+16$	7.23	$6.68\text{E}+15$
$M = 0.2$	$5.81\text{E}+16$	5.35	$1.33\text{E}+16$
$M = 0.1$	$1.14\text{E}+17$	3.56	$2.61\text{E}+16$
$M = 0.05$	$2.11\text{E}+17$	1.87	$4.40\text{E}+16$
		0.26	$7.88\text{E}+16$
		-0.28	$9.65\text{E}+16$

Experimental (CER)  $\Delta n_c^{\text{sep}} \sim 2 \times 10^{16} \text{ C}/\text{m}^3$ .

the four control parameters. Table 1 shows,  $\Delta n_c^{\text{sep}}$ , (total all ion charge states) for each of these simulations. The experimentally measured value of  $\Delta n_c^{\text{sep}}$  is  $\sim 2.0 \times 10^{16} \text{ C}/\text{m}^3$ , from charge exchange recombination spectroscopy (CER) measurements.  $M_{\parallel} \sim 0.3\text{--}0.6$  and  $\Delta r_s \sim +3.6 \text{ cm}$  are consistent with the total amount of carbon entering the core plasma as well as the deposition pattern. The calculated  $\Delta n_c^{\text{sep}}$  is not very sensitive to the assumed value of  $D_{\perp}$ , thus more tightly identifying the value of  $M_{\parallel}$ . For the majority of cases there is little or no deposition anywhere but in the inner divertor region. The only exception was for  $M_{\parallel} = 0.05$  where  $\sim 25\%$  of the particles deposited on the inner wall and  $\sim 8\%$  on the outer target.

### 3. Discussion

The foregoing analysis constitutes a first, simple treatment. It nevertheless appears adequate to identify approximate values for the four main control parameters. The inferred  $M_{\parallel} \sim 0.4$  and radial location of the  $\text{C}^+$ -source agrees with analysis of the CII and CIII intensity distributions near the gas inlet measured by tangential viewing cameras [6].  $M_{\parallel} \sim 0.4$  is also in accord with the values inferred from modeling of the co-deposition in the JET DT campaign as well as directly measured with Mach probes on JET [8] and JT-60U [9]. It is evident that this still unexplained, fast SOL flow is an effect governing the carbon transport and deposition processes in divertor tokamaks.

A number of refinements will be included in future work. A potentially important effect, which has not been included in the present analysis, is the erosion and re-

deposition of the  $^{13}\text{C}$  particles which strike the inner target – i.e. the redistribution of the  $^{13}\text{C}$  resulting from the ongoing plasma exposure. Preliminary modeling of the erosion and re-deposition patterns at the inner target indicates that this is a net deposition region, which tends to justify the neglect of erosion and re-deposition for the *present* case. This simplifying aspect of the present experiment cannot be expected generally. In the JET (largely strongly beam-heated) DT campaign, the carbon ( $^{12}\text{C}$ ) that initially arrived at the inner target did not stop there but continued on to deposit on adjacent surfaces that were out of plasma contact [8]. However, the JET  $^{13}\text{C}$ –methane experiments [2] were, as here, done in L-mode and in that case little additional transport by erosion and re-deposition was seen in the divertor. The rather low input power of the present L-mode SAPP experiment has resulted in this very valuable simplification. In future studies, erosion and re-deposition are likely to play a more important – and possibly totally dominating – role.

The fact that the injection of the methane was toroidally symmetric greatly aided the interpretation of the C deposition, not least because the OEDGE analysis code, like most edge codes, is 2D.

#### 4. Conclusions

This study identified and quantified four control variables governing the  $^{13}\text{C}$  deposition and core contamination behaviour: (a)  $\sim 50 \pm 20\%$  conversion efficiency of  $^{13}\text{CH}_4$  to  $^{13}\text{C}^+$ , (b)  $^{13}\text{C}^+$  source  $\sim 3\text{--}6$  cm outboard of the separatrix near the  $^{13}\text{CH}_4$  injection location, (c)  $D_{\perp} \sim 0.3\text{--}0.5 \text{ m}^2\text{s}^{-1}$ , (d)  $M_{\parallel} \sim 0.3\text{--}0.6$  toward inside. There is no evidence, for the plasma conditions involved in the present study, of substantial erosion and re-depo-

sition of the  $^{13}\text{C}$ . It thus constitutes the simplest possible case and provides a valuable basis on which to proceed to the general case where redistribution of the initial deposition pattern occurs by ongoing plasma impact.

#### Acknowledgments

The authors would like to acknowledge the support of a Collaborative Research Opportunities Grant from the Natural Sciences and Engineering Research Council of Canada and the US D.O.E. This work was supported in part by the US Department of Energy under DE-FC02-04ER54698, W-7405-ENG-48, DE-FG03-96ER54373, DE-FG02-04ER54758, and DE-AC04-94AL85000.

#### References

- [1] P. Wienhold, H.G. Esser, D. Hildebrandt, et al., *J. Nucl. Mater.* 290–293 (2001) 362.
- [2] J. Likonen, S. Lehto, J.P. Coad, et al., *Fus. Eng. Des.* 66–68 (2003) 219.
- [3] S.L. Allen, A.G. McLean, W.R. Wampler, et al., these Proceedings, doi:10.1016/j.jnucmat.2004.09.066.
- [4] W.R. Wampler, S.L. Allen, A.G. McLean, et al., these Proceedings, doi:10.1016/j.jnucmat.2004.10.124.
- [5] P.C. Stangeby, J.D. Elder, J.A. Boedo, et al., *J. Nucl. Mater.* 313–316 (2003) 883.
- [6] A.G. McLean, J.D. Elder, P.C. Stangeby, et al., these Proceedings, doi:10.1016/j.jnucmat.2004.10.130.
- [7] S. Lisgo, P.C. Stangeby, J.D. Elder, et al., these Proceedings, doi:10.1016/j.jnucmat.2004.09.055.
- [8] J.P. Coad, N. Bekris, J.D. Elder, et al., *J. Nucl. Mater.* 290–293 (2001) 224.
- [9] N. Asakura, H. Takenaga, S. Sakurai, et al., *Plasma Phys. Control. Fus.* 44 (2002) 2101.